Seasonal prediction of US summertime ozone using statistical analysis of large scale climate patterns

Lu Shen[a,1] and Loretta J. Mickley[a]

[a]John A. Paulson School of Engineering and Applied Sciences, Harvard University, Cambridge, MA 02138

Edited by Guy Brasseur, Max Planck Institute of Meteorology, Hamburg, Germany, and accepted by Editorial Board Member A. R. Ravishankara January 10, 2017 (received for review June 30, 2016)

We develop a statistical model to predict June–July–August (JJA) daily maximum 8-h average (MDA8) ozone concentrations in the eastern United States based on large-scale climate patterns during the previous spring. We find that anomalously high JJA ozone in the East is correlated with these springtime patterns: warm tropical Atlantic and cold northeast Pacific sea surface temperatures (SSTs), as well as positive sea level pressure (SLP) anomalies over Hawaii and negative SLP anomalies over the Atlantic and North America. We then develop a linear regression model to predict JJA MDA8 ozone from 1980 to 2013, using the identified SST and SLP patterns from the previous spring. The model explains ∼45% of the variability in JJA MDA8 ozone concentrations and ∼30% variability in the number of JJA ozone episodes (>70 ppbv) when averaged over the eastern United States. This seasonal predictability results from large-scale ocean–atmosphere interactions. Warm tropical Atlantic SSTs can trigger diabatic heating in the atmosphere and influence the extratropical climate through stationary wave propagation, leading to greater subsidence, less precipitation, and higher temperatures in the East, which increases surface ozone concentrations there. Cooler SSTs in the northeast Pacific are also associated with more summertime heatwaves and high ozone in the East. On average, models participating in the Atmospheric Model Intercomparison Project fail to capture the influence of this ocean–atmosphere interaction on temperatures in the eastern United States, implying that such models would have difficulty simulating the interannual variability of surface ozone in this region.

ozone | seasonal forecast | teleconnection | sea surface temperature

In response to air quality regulations, levels of surface ozone over the United States have declined in recent years (1). However, the year-to-year variability in surface ozone is still quite large and can have important consequences for public health (e.g., ref. 2). For example, the extreme heat in the central United States in summer 2012 coincided with an enhanced number of ozone exceedances in Midwestern cities like St. Louis, compared with the previous 3–4 y (3). Prior knowledge of summertime ozone concentrations in the previous spring [March–April–May (MAM)] would be useful for air quality management. Given the dependence of surface ozone on meteorological variables and the links between large-scale circulation patterns and regional weather, such prior knowledge seems feasible. This study explores the teleconnections between surface ozone in the eastern United States and large-scale circulation patterns as defined by patterns in sea surface temperatures (SSTs) and sea level pressures (SLPs). We develop a statistical model to predict summertime ozone in the eastern United States during the previous spring, and we evaluate the capability of chemistry–climate models to capture the teleconnections identified here as important to US ozone.

High-ozone episodes occur in response to high surface temperatures, low wind speeds, clear skies, subsidence from aloft, and stagnant conditions (4, 5), and these relationships may vary under different meteorological conditions due to the nonlinear response of ozone to chemistry and meteorology. Although changes in the emissions of ozone precursors can strongly affect surface ozone air quality (e.g., ref. 6), the interannual variability in weather is much greater than that in anthropogenic emissions (7). Here, we exploit the dependence of surface ozone on weather in an effort to predict summertime ozone one season in advance. Achieving our goal depends on how much memory the ocean–atmosphere system can retain from spring to summer. Sea heat content, as quantified by SSTs, has a relatively long inertial memory of months to years, and SST anomalies may excite large-scale circulation patterns in the atmosphere (e.g., refs. 8 and 9). Previous studies have linked precipitation and drought frequency in the United States to such large-scale phenomena as El Niño (10–13), the Pacific Decadal Oscillation (12, 14), and the Atlantic Multidecadal Oscillation (AMO) (14–17). Heatwave frequency in the United States is affected by changes in greenhouse gas content (e.g., ref. 18), soil moisture, and local precipitation (19–21), as well as by patterns in SSTs in both Pacific and Atlantic Ocean (16, 17, 22–24). These relationships imply that ozone is also likely to be influenced by these large-scale climate patterns and can be predicted in advance.

Both statistical and dynamical models can be used for the seasonal prediction of atmospheric variables. Statistical models include linear correlation models, eigen techniques, and nonlinear methods (25, 26). A commonly used statistical tool is the canonical correlation analysis, which finds the empirical relationship between two spatial patterns based on the covariability between them. Such analysis has been used to predict precipitation (e.g., refs. 8 and 27) and temperature (e.g., ref. 19). However, compared with meteorological observations, which can be available on timescales approaching 100 y, the period with ozone observations

Significance

This study identifies the relationship between summertime ozone air quality in the eastern United States and large-scale meteorological patterns, including sea surface temperature (SST) patterns and teleconnections, evolving over the preceding months. We show that this relationship can be used in spring to predict ozone for the following summer. Our work implies that large-scale phenomena such as the Atlantic Multidecadal Oscillation may drive multidecadal variability in US ozone air quality. We find in particular that springtime tropical Atlantic SSTs have a significant influence on summertime meteorology and ozone air quality in the eastern United States, but the free-running, atmosphere-only climate models with prescribed SSTs fail to capture these seasonally evolving teleconnections.

Author contributions: L.S. and L.J.M. designed research; L.S. performed research; L.S. analyzed data; and L.S. and L.J.M. wrote the paper.

The authors declare no conflict of interest.

This article is a PNAS Direct Submission. G.B. is a Guest Editor invited by the Editorial Board.

Freely available online through the PNAS open access option.

Data deposition: The replication data reported in this paper have been deposited in the Harvard Dataverse, https://dataverse.harvard.edu (digital object identifier no. 10.7910/DVN/BM8N4C).

[1]To whom correspondence should be addressed. Email: lshen@fas.harvard.edu.

This article contains supporting information online at www.pnas.org/lookup/suppl/doi:10.1073/pnas.1610708114/-/DCSupplemental.

is relatively short, only ~30 y in the United States. Dynamical forecasts using a climate model provide an alternative way to predict surface ozone one season ahead. Such models do not depend on historical observations, but they may not be able to replicate important interannual and decadal phenomena in both the atmosphere and ocean (26). In addition, dynamical forecasts of ozone require the use of chemistry transport models, which often overestimate summertime ozone concentrations in the eastern United States (28, 29) and may fail to capture the ozone-temperature slopes (e.g., ref. 30) due to uncertainty in ozone-isoprene chemistry (e.g., ref. 28) as well as emissions (e.g., ref. 31). In this study, we develop a linear model based on teleconnections between surface ozone and SST/SLP anomalies to predict the summertime ozone in the previous spring.

Correlation of June–July–August Ozone with Evolving Patterns of SST/SLP

We first apply empirical orthogonal functions (EOFs) to decompose the seasonal variability of mean June–July–August (JJA) daily maximum 8-h average (MDA8) ozone in the eastern United States over 1980–2013. We find that the spatial loadings of the first EOF (EOF1) are mainly located north of 31°N (*SI Appendix*, Fig. S1) and that this EOF explains 47% of total variance. Previous work has shown that EOF1 is associated with the north-south movement of polar jet wind in summer (32). Given that EOF1 explains so much ozone variance, this paper focuses on identifying those large-scale patterns in springtime SST and SLP that influence ozone in the region of EOF1 maximum loadings (100°W to 65°W, 31°N to 50°N; the quadrangle in Fig. 1*A*). Hereafter, we use the term "East-JJA-O_3" to refer to the average JJA MDA8 ozone in the eastern United States, north of 31°N.

We find that the combination of anomalously warm SSTs in the northern Atlantic Ocean and cold SSTs in the northeast Pacific provides a potential source of seasonal predictability for East-JJA-O_3. Fig. 1 *A*–*C* shows the correlation coefficient *r* of East-JJA-O_3 and SST in the seasons leading up to and including summer over the 1980–2013 time period. In all seasons, we find negative correlations north of 10°N in the northeast Pacific (Fig. 1 *A*–*C*), indicating that this teleconnection with ozone is likely independent of the El Niño–Southern Oscillation, which has its most pronounced signal in the tropical Pacific. In spring and summer, the northern Atlantic Ocean displays a tripole mode, with positive correlations between East-JJA-O_3 and SSTs in the tropics and high latitudes but negative correlations in the midlatitudes (Fig. 1 *B* and *C*). The warm Atlantic ocean can act as a diabatic "pump" to alter atmospheric circulation, leading to ascent of air over the northern Atlantic (0° to 50°N) and descent in the northeast Pacific and United States (16, 17). Fig. 1 reveals that the observed SST patterns that correlate with East-JJA-O_3 develop over time, from winter to summer, and that the regions with significant correlations expand. To characterize this SST pattern, we define MAM-ΔSST as the average SST difference between the tropical northern Atlantic Ocean (black rectangle in Fig. 1*B*) and the northeastern Pacific Ocean (red rectangle in Fig. 1*B*) in spring. Fig. 1*C* also shows a dipole pattern in the northeastern Pacific in summer, characterized by negative correlations stretching along the west coast of North America and by positive correlations in the central Pacific. This pattern resembles the Pacific extreme pattern (PEP), as identified by McKinnon et al. (24), who found that it is associated with more heatwaves in the eastern United States.

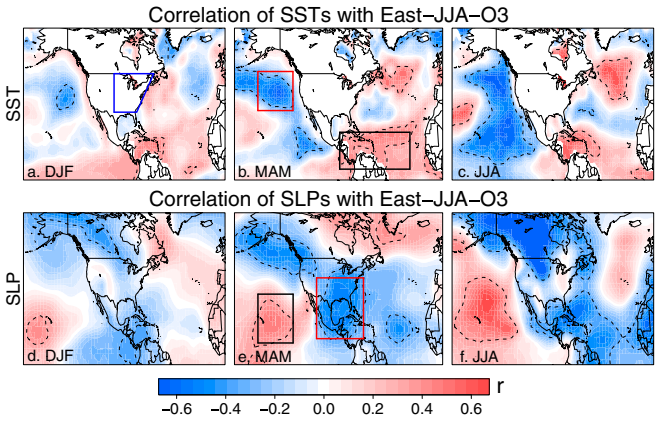

Fig. 1. Correlations of mean JJA MDA8 ozone in the eastern United States (East-JJA-O_3) with seasonal mean SSTs (*A*–*C*) and SLPs (*D*–*F*) for the seasons leading up to and including summer for 1980–2013. The blue quadrangle in *A* indicates the domain of East-JJA-O_3. The dashed contour lines enclose regions in which the correlations reach statistical significance ($P < 0.05$). We define the MAM-ΔSST index as the average difference in MAM SSTs between the northern tropical Atlantic ocean (black rectangle in *B*) and the northeastern Pacific ocean (red rectangle) and the MAM-ΔSLP index as the average difference in MAM SLP between the eastern Pacific (black rectangle in *B*) and a large region including much of the eastern and central United States, Mexico, and the Gulf of Mexico (red rectangle). SSTs are from ERSST v3b. Meteorological data are from NCEP. Ozone data are from the EPA Air Quality System. All data are detrended by subtracting the 7-y MAs.

As with SST, the influence of SLP on East-JJA-O_3 displays a distinctive pattern across the Atlantic and Pacific Oceans. Fig. 1 *D*–*F* shows the 1980–2013 correlation coefficient *r* of East-JJA-O_3 and SLP in the seasons leading up to and including summer. The correlations reveal a bimodal structure with positive values over the eastern Pacific between 10°N and 30°N and negative values extending across the tropical and northern Atlantic, much of North America, and the northeastern Pacific. Previous research has suggested that anomalously low SLPs in the Atlantic Ocean may weaken the Bermuda High (33). Here, we define MAM-ΔSLP as the average SLP difference between the eastern United States/Gulf of Mexico (black rectangle in Fig. 1*E*) and the eastern Pacific Ocean (red rectangle in Fig. 1*E*) in spring.

By examining the covariance of meteorological fields in spring and summer (*SI Appendix*, Table S1 and Fig. S2), we infer that the observed influence of SSTs and SLPs on East-JJA-O_3 (Fig. 1) actually reflects the variability of atmospheric circulations over a much larger domain, including the northeast Pacific, North America, and the North Atlantic. This result suggests that the variability of seasonal ozone in the eastern United States arises in part from large-scale ocean–atmosphere interactions and is likely to be predicted in advance.

Prediction of JJA Ozone in the Eastern United States Using SST and SLP

We develop the statistical prediction model by regressing the 1980–2013 time series of East-JJA-O_3 onto the two metrics, MAM-ΔSST and MAM-ΔSLP. Fig. 2 *A* and *B* reveal that both of these metrics are correlated with ozone variability across much of the eastern United States, with MAM-ΔSST accounting for correlations with JJA ozone as high as ~0.7. MAM-ΔSLP has less influence over the Gulf region than MAM-ΔSST. We test three regression models for ozone in each grid box, defined as

$$ozone = f(\text{MAM-}\Delta\text{SST, MAM-}\Delta\text{SLP}), \quad [1]$$

$$ozone = f(\text{MAM-}\Delta\text{SST}), \quad [2]$$

$$ozone = f(\text{MAM-}\Delta\text{SLP}), \quad [3]$$

where *ozone* denotes mean JJA MDA8 ozone. To avoid overfitting and to identify the best model for each grid box, we use leave-one-out cross-validation. In each grid box, we use one observation in the time series as the test data point and the remaining ones as the training set, and we repeat this process until all observations have been predicted. Using this method, we find that Eq. **1** is the best model in the Midwest and part of Northeast, Eq. **2** is best in the Southeast and the rest of the Northeast, and Eq. **3** is best in the Great Plains. The correlation coefficient *r*

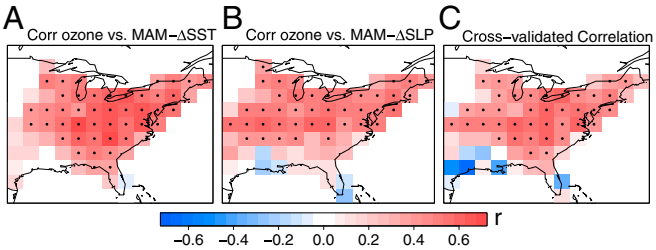

Fig. 2. Correlation of mean JJA MDA8 ozone in each grid box with the MAM-ΔSST (*A*) and MAM-ΔSLP (*B*) indices for 1980–2013. The two indices are defined in Fig. 1. *C* shows the cross-validated correlation coefficient *r* between observed and modeled mean JJA MDA8 ozone. The modeled ozone uses MAM-ΔSST in the Southeast and part of the Northeast, MAM-ΔSLP in the Great Plains, and a combination of both in the Midwest and part of the Northeast. The ozone time series has been detrended by subtracting the 7-y MA. In *A*–*C*, grid boxes with statistically significant ($P < 0.05$) correlations are stippled.

of observed and predicted MDA8 ozone is ∼0.6 in the Southeast and Northeast and ∼0.5 in the Midwest (Fig. 2*C*).

Fig. 3 compares the 1980–2013 time series of observed and predicted JJA MDA8 ozone anomalies averaged over the eastern United States. The time series are detrended using two different approaches, as described in *Materials and Methods*. We find that using a 7-y moving average (MA) to detrend the time series in both ozone and meteorology yields a correlation coefficient *r* of 0.59 between observed and predicted ozone values. Using the seven-term Henderson filtered (HF) average to detrend the time series yields a higher correlation coefficient of 0.67, suggesting that this method can better deal with abrupt changes in the time series. These results imply that we can predict about 45% of the JJA MDA8 ozone variability in the eastern United States in the previous spring. We also investigate the potential of our approach to predict the number of JJA ozone episodes, which we define as days each summer when MDA8 ozone exceeds 70 ppbv in a 2.5° × 2.5° grid box. We use the same regression method as above but replace SLP with 500-hPa geopotential heights because this variable is better correlated with ozone episodes than is SLP (*SI Appendix*, Figs. S3–S6). For the 1980–2013 time series of ozone episode number averaged over the eastern United States, we find correlations between observations and predictions of 0.52–0.55, depending on the detrending method (*SI Appendix*, Fig. S7). Thus, the model can predict as much as 30% of the variability in summertime ozone episodes in the preceding spring.

Physical Mechanism for the SST/SLP Relationships with US MDA8 Ozone

In their model study focused on impacts of the AMO, Sutton and Hodson (16, 17) found that diabatic heating drives the large-scale climate response to warming and cooling of the tropical north Atlantic Ocean. Consistent with Gill (34), these authors reported that anomalously warm tropical Atlantic SSTs induce ascent over the Atlantic and lead to a pattern of low SLPs extending from Atlantic to North America. Taken together, these results suggest that summertime ozone in the eastern United States is closely related to tropical Atlantic SST variability. The vertical motion is associated with cyclonic circulation in the lower troposphere over southern North America and anticyclonic circulation aloft. Over the eastern United States, these circulation anomalies can lead to increased surface temperatures, enhanced subsidence, and reduced precipitation.

By testing correlations of different meteorological variables with tropical north Atlantic SSTs, we provide additional evidence in support of the mechanism identified by Sutton and Hodson (16, 17). First, we find that the warm tropical Atlantic SSTs in spring correlate with cold SSTs in the central Atlantic and central Pacific, both in spring and in the following summer (Fig. 4*A* and *SI Appendix*, Fig. S8*A*). Second, we find that spring surface air temperatures over much of the Intermountain West and part of the southeastern United States are anti-correlated with spring tropical Atlantic SSTs (*SI Appendix*, Fig. S8*C*), whereas the summertime surface air temperatures in the East are highly correlated with spring tropical Atlantic SSTs (Fig. 4*C*). As observed by Sutton and Hodson (16, 17), we see negative correlations between SSTs and SLPs over much of North America and the north Atlantic (Fig. 4*E* and *SI Appendix*, Fig. S8*E*). Finally, warm SST anomalies in the tropical north Atlantic in spring are associated with decreased 300-hPa geopotential heights over the eastern United States in spring (*SI Appendix*, Fig. S8*G*) and increased geopotential heights over the eastern and central United States the following summer (Fig. 4*G*). Taken together, these processes in the eastern United States [i.e., warmer temperatures, greater subsidence accompanied by clear skies in the Northeast and Mid-Atlantic States, as well as reduced precipitation over much of the East (*SI Appendix*, Fig. S9)] tend to increase surface ozone in summer and lead to more frequent ozone episodes.

Consideration of the variability in North Pacific SSTs improves the predictability of summertime ozone in the eastern United States (*SI Appendix*, Fig. S10). Using correlation analysis, we find that cool North Pacific SSTs persist from spring to summer (Fig. 4*B* and *SI Appendix*, Fig. S8*B*), similar to the evolving patterns of correlations between North Pacific SST and summertime ozone in the eastern United States (Fig. 1 *B* and *C*). The fully developed dipole pattern in JJA SSTs, characterized by a negative anomaly stretching along the west coast of North America and by a positive anomaly in the central Pacific (Figs. 1*C* and 4*B*), resembles the PEP (24), which can provide skillful predictions of extreme summer temperatures across the eastern United States as many as 50 d in advance (24). The PEP is associated with an eastward-propagating flux in wave activity that tends to increase surface pressures and reduce precipitation across the eastern United States, resulting in warmer surface temperatures (Fig. 4*D*), more frequent heat waves (24), and enhanced ozone concentrations (Fig. 1*C*). Cool northeast Pacific SSTs (Fig. 4*B*) are also concurrent with anomalous high SLPs in the central Pacific and low SLPs over the North Pacific and Atlantic (Fig. 4*F*), as well as increased 300-hPa geopotential heights in summer (Fig. 4*H*). This combination of phenomena is consistent with the teleconnection pattern associated with enhanced ozone in the East (Fig. 1), and the North Pacific SSTs exhibit an even stronger correlation with the East-JJA-O_3 than the tropical Atlantic SSTs (*SI Appendix*, Fig. S10).

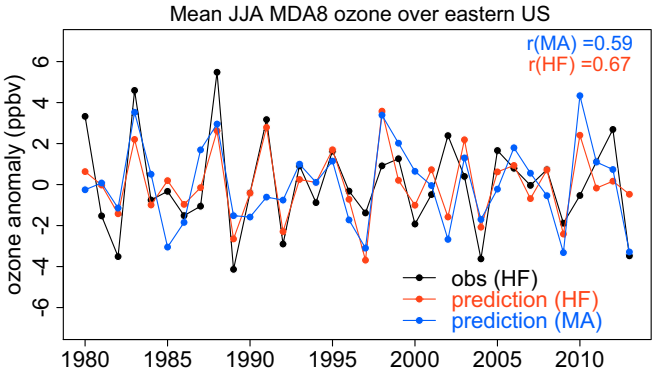

Fig. 3. Time series of observed and modeled mean JJA MDA8 ozone, averaged over the eastern United States (100°W to 65°W, 31°N to 50°N). Observations are shown in black and are detrended using 7-y Henderson filtered average (HF). The red curve denotes the modeled values detrended using HF, whereas the blue curve indicates modeled values detrended using the 7-y MA. The correlations *r* of the two modeled time series with that observed are shown (*Inset*).

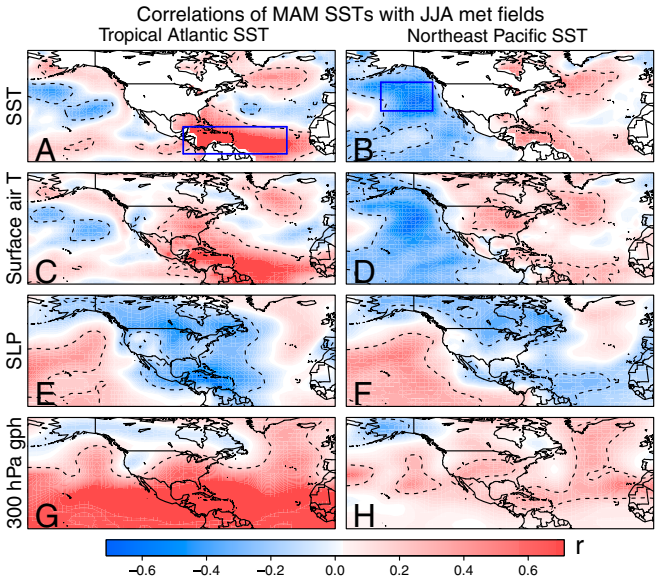

Fig. 4. (*A*) Correlations of mean MAM tropical Atlantic SSTs, averaged over the ocean grid boxes in the blue rectangle in *A*, with SSTs in summer for 1948–2013. *B* is the same as *A* but uses mean MAM northeast Pacific SSTs, averaged over the ocean grid boxes in the blue rectangle in *B*. *C* and *D* are correlations with surface air temperatures, *E* and *F* with SLP, and *G* and *H* with 300-hPa geopotential heights (gph). The dashed contour lines enclose regions in which the correlations are statistically significant ($P < 0.05$). To easily compare with Fig. 1 and with *A*, *C*, *E*, and *G*, we have reversed the sign of correlations in *B*, *D*, *F*, and *G*. All data are detrended by subtacting the 7-y MAs.

Unlike SSTs in the tropical Atlantic, SSTs in the North Pacific are more likely to respond to large-scale atmospheric variability than to serve as a "trigger" to such variability. We apply EOF analysis to the mean springtime SSTs in the northeast Pacific (60°N to 20°N, 180°W to 100°W), the same region as used by Johnstone and Mantua (35), from 1948 to 2013. The leading EOF mode (EOF1) explains 33.8% of the total variances, displaying an arc-like structure with positive anomaly stretching around the North America west coast (*SI Appendix*, Fig. S11*A*). Using multiple independent data sources, Johnstone and Mantua (35) demonstrated that SLP patterns drive more than half the variance of EOF1 in northeast Pacific SSTs. The second EOF mode (EOF2) explains 18.1% of the total variance, featuring a negative anomaly in the central northeast Pacific (*SI Appendix*, Fig. S11*B*), a pattern sometimes referred to as "The Blob" (36). SSTs in the central northeast Pacific in Fig. 1*B*, which we use to predict summertime ozone in the eastern United States, also correlate strongly with the SST EOF2 time series ($r = 0.84$). In a case study, Bond et al. (36) demonstrated that the SST warm anomaly during the winter of 2013–2014 was caused by anomalously high SLPs in that region, which suppressed the loss of heat from ocean to atmosphere and decreased cold advection in the upper ocean. In our correlation analysis, we find that cool central northeast Pacific SSTs are concurrent with low SLPs in the same general region (*SI Appendix*, Fig. S8 *B* and *F*), consistent with Bond et al. (36).

Evaluation of Teleconnections in Other Datasets and the Atmospheric Model Intercomparison Project Models

Here, we evaluate the capability of the 20th Century Reanalysis, the Atmospheric Model Intercomparison Project (AMIP) models, and other model datasets to capture the observed links between mean JJA temperatures in the eastern United States (East-JJA-T) and patterns in SST/SLP, as described in *Materials and Methods*. Unlike the National Centers for Environmental Prediction (NCEP) Reanalysis, the 20th Century Reanalysis assimilates only observed surface pressures, SSTs, and sea ice. The AMIP models are particularly suited for this exercise as they are forced only by observed, monthly mean SSTs and sea ice extent (37). We carry out these evaluations by regressing multidecadal time series of East-JJA-T onto the SST fields in spring and summer, with surface temperatures averaged over the same domain as East-JJA-O_3.

Fig. 5 *A* and *B* shows the correlation coefficient *r* of East-JJA-T from the NCEP Reanalysis and SSTs over the northeast Pacific and North Atlantic in spring and summer. The figure displays a spatial pattern similar to that for ozone in Fig. 1 *B* and *C*, with a tripole mode in the Atlantic and negative correlations in the northeast Pacific and US west coast in both seasons. Fig. 5 *C* and *D* are the same as Fig. 5 *A* and *B*, but using the 20th Century Reanalysis, which again resembles the correlation pattern of East-JJA-O_3 and springtime SSTs (Fig. 1*B*). Fig. 5 *E* and *F* show the median correlations between East-JJA-T and seasonal SSTs in the 28 AMIP models (*SI Appendix*, Table S2) for 1979–2008. In spring, most AMIP models yield positive correlations between East-JJA-T and SSTs in the Atlantic and negative correlations in the Pacific, but the correlations are much weaker than those in NCEP and the 20th Century Reanalysis, with large differences in the spatial patterns (Fig. 5*E*). Unlike correlations in the other datasets, those in the AMIP simulations are insignificant in the tropical Atlantic. In summer, the AMIP models show a tripole pattern, but the correlation in the southernmost pole over the tropical Atlantic is very weak and the northernmost pole shifts from the high-latitudes (>50°N), as seen in the NCEP Reanalysis, to the midlatitudes (35°N to 50°N; Fig. 5*F*). The correlation patterns between East-JJA-T and seasonal SSTs for each AMIP model can be found in *SI Appendix*, Figs. S12–S13. We further calculate the EOFs of JJA surface air temperature over North America and surrounding oceans for 1979–2008 in both NCEP Reanalysis and all AMIP models. Results suggest that the AMIP models cannot fully reproduce the observed EOF patterns of summertime temperature over North America and surrounding oceans (*SI Appendix*, Figs. S14–S17).

We also regress East-JJA-T onto the SLP in spring and summer. For both NCEP and the 20th Century Reanalysis, we find

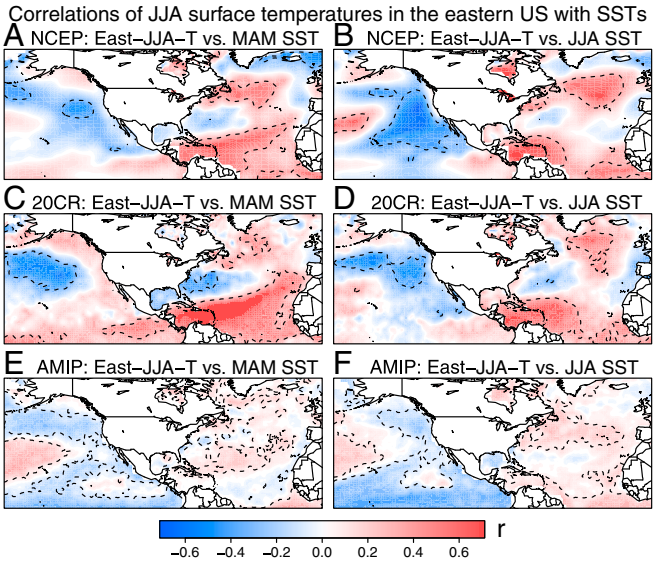

Fig. 5. Correlations of mean JJA surface air temperatures averaged over the eastern United States (100°W to 65°W, 31°N to 50°N; quadrangle in Fig. 1) with SSTs for spring and summer over 1979–2008. *A* and *B* present the correlations in the NCEP Reanalysis 1 with ERSST v3b, *C* and *D* in the 20th Century Reanalysis with HadISST, and *E* and *F* in the ensemble of 28 AMIP models with SSTs from Taylor et al. (42). The dashed contour lines enclose regions in which the correlations are statistically significant ($P < 0.05$) for NCEP and the 20th Century Reanalysis or where at least 20 models in the AMIP ensemble yield the same sign in correlation coefficient. All data are detrended by subtracting the 7-y MAs.

positive correlations in the central northeast Pacific and negative correlations extending from the Atlantic, across the United States, and to the northeast Pacific (*SI Appendix*, Fig. S18 *A–D*). The patterns of spatial correlation of SLPs and summertime temperatures in the East look very different in the AMIP models (*SI Appendix*, Fig. S18 *E* and *F*), with positive correlations across the northeastern Pacific, parts of North America, and the Atlantic in spring. The correlations strengthen in the Pacific in summer, as in the other two datasets, but the negative correlations are relatively weak over the Atlantic.

We then investigate whether the climate models capture the influence of tropical Atlantic forcing on US surface air temperature given enough integrating time. Sutton and Hodson (16, 17) found that prescribing SSTs typical of the warm and cold phases of AMO over ∼20 y led to surface temperature differences between the two phases of 0.25–0.75 K across the eastern United States, with warmer temperatures mainly driven by warming in the tropical Atlantic (0°N to 30°N). We repeat this experiment using the Goddard Institute for Space Studies (GISS) ModelE2, following Sutton and Hodson (16, 17), as described in *SI Appendix*. Results in ModelE2 show a 0–0.6 K warming over the East in response to tropical SST warming (*SI Appendix*, Fig. S19). More evidence of the influence of tropical Atlantic SSTs is provided by idealized experiments from the US Climate Variability and Predictability Program (CLIVAR) drought-working group. To compare these results with those from ModelE2 and Sutton and Hodson (16, 17), we scale the results from National Center for Atmospheric Research (NCAR) Community Atmosphere Model version 3.5 (CAM3.5) and Geophysical Fluid Dynamics Laboratory (GFDL) Atmospheric Model version 2.1 (AM2.1) so that the surface air temperature response corresponds to a ∼0.25 K warming in the tropical Atlantic Ocean (88°W to 13°W, 10°N to 20°N). In the CLIVAR models, the SST forcing is confined to 10°N to 20°N, whereas the SST forcing in Sutton and Hodson (16, 17) and in ModelE2 spans over 0°N to 30°N with an average warming of 0.25 K between 10°N to 20°N (*SI Appendix*, Figs. S19*A* and 20*A*). The CLIVAR models show a warming across the eastern United States associated with elevated tropical Atlantic SSTs after integrating for 51 y, but the pattern of the warming differs among models. CAM3.5 displays 0.1–0.5 K warming response over the central and eastern United States (*SI Appendix*, Fig. S20*B*). AM2.1 shows 0.1–0.4 K warming in the Great Plains and Southeast, but minimal response elsewhere (*SI Appendix*, Fig. S20*C*). Results from all three models are comparable to the observed differences between cold to warm AMO years in Sutton and Hodson (16, 17).

Our results imply that given sufficient integrating time, climate models can indeed capture the response of JJA air temperature in the eastern United States to the variability in tropical Atlantic SSTs. However, it is not clear why US surface temperatures in the models respond only weakly or not at all to SST forcing on timescales of months (Fig. 5 *E* and *F*), even though this is a clear feature in the observations. Similar problems regarding ocean-land-atmosphere interactions have been reported in other studies (e.g., ref. 35). Results from the 20th Century Reanalysis suggest that this model deficiency may be addressed by assimilating not just observed SSTs but also the observed SLP patterns.

Conclusions

This study presents a statistical model for springtime prediction of ozone pollution in the eastern United States during the following summer. The model exploits observed relationships between JJA MDA8 ozone in the eastern United States (East-JJA-O_3) and meteorological patterns evolving over the preceding months. We find that anomalously high JJA ozone concentrations in the East are linked to warm tropical Atlantic and cold northeast Pacific SSTs during the preceding spring, concurrent with positive SLP anomalies around Hawaii and negative SLP anomalies over the Atlantic and North America.

Our statistical model uses two predictors, the SST difference between the northeast Pacific and tropical Atlantic and the SLP difference between Hawaii and the eastern United States/ Gulf of Mexico in the preceding spring. The cross-validated model predicts 45% of the 1980–2013 variability in East-JJA-O_3 and ∼30% variability in the number of JJA ozone episodes (≥70 ppbv) averaged over the eastern United States. This prediction can be made in the early June once the MAM averaged SLP and SST are available. Earlier predictions are also possible if we use predictors averaged in earlier months. There are several difficulties in further improving the seasonal predictive capability of JJA ozone concentration. First, the history of ozone observations (∼34 y) is much shorter than that of the meteorological variables, which prohibits the use of a more complicated model (e.g., canonical correlation analysis). Second, ozone chemistry is complex and responds nonlinearly to meteorology and anthropogenic emissions (e.g., ref. 4), making predicting ozone relatively challenging. Third, surface ozone is also influenced by short-term natural variability, on the order of days to weeks. Given these challenges, whether the predictability of seasonal ozone will increase or decrease in the cleaner environment of the future is unclear (*SI Appendix*, Figs. S21–S24). The application of this seasonal forecast model in air quality planning also requires an appropriate assumption of ozone precursor trends, which can affect the detrending approaches of ozone time series (*SI Appendix*, Fig. S25).

Previous studies have suggested that the frequency of US heat waves is affected by a range of variables, including the variability in both Pacific and Atlantic Ocean SSTs (22–24). In this study, we find that the source of seasonal predictability for JJA MDA8 ozone in the eastern United States relies on large-scale ocean–atmosphere interactions. The warming of tropical Atlantic SSTs can trigger diabatic heating in the atmosphere, inducing ascent over the Atlantic and decreasing SLP in a swath extending across the Atlantic to North America (16, 17). This pattern of SSTs and SLPs perturbs the extratropical climate through the propagation of stationary waves, leading to increased surface temperature, enhanced subsidence and reduced precipitation in the eastern United States. In response to the atmospheric perturbation, cool northeast Pacific SSTs can persist from spring to summer, developing into the PEP. The PEP, in turn, is associated with an eastward-propagating flux in wave activity that tends to increase surface pressure and reduce precipitation in the eastern United States, resulting in more frequent heat waves (24) and enhanced ozone concentrations.

We evaluate whether climate models can capture the observed interannual variability in US surface temperatures and, more specifically, whether they can reproduce the positive correlations between JJA surface air temperatures in the East and tropical Atlantic SSTs. To that end, we test a suite of models participating in the AMIP. We find that the AMIP models, forced by observed SSTs and sea ice extent, greatly underestimate the correlation of JJA temperatures in the East with SSTs in both Atlantic and Pacific Ocean. Our results indicate the challenges for freely running climate models attempting to simulate the variability in not just US surface temperatures, but also in MDA8 ozone, which is strongly dependent on temperature.

Finally, by diagnosing links between US ozone and SST patterns, our study implies that large-scale phenomena such as AMO may drive multidecadal variability in US ozone air quality, an influence which has not yet been investigated. Such phenomena are typically overlooked in both model and observational analyses of past ozone trends and model projections of future ozone levels (e.g., ref. 5).

Materials and Methods

Hourly surface ozone concentrations are obtained from the Environmental Protection Agency (EPA) Air Quality System (https://www3.epa.gov/ttn/airs/airsaqs) from 1980 to 2013. We convert hourly ozone data to MDA8 ozone and then interpolate to 2.5° × 2.5° spatial resolution by averaging all of the sites with more than 40% coverage over the 1980–2013 JJA days within each

grid cell. We also use the 1948–2013 meteorological data from the NCEP Reanalysis 1 (38), which assimilates a variety of observations and is used in many previous studies. The dataset also has a spatial resolution of 2.5° × 2.5° and includes SLP, geopotential height, and surface air temperature.

As part of this study, we compare our results using NCEP Reanalysis with those using the 20th Century Reanalysis (v2). This reanalysis spans from 1871 to 2012, and unlike the NCEP dataset, assimilates only surface pressure and uses SST and sea ice distributions as boundary conditions (39). The 20th Century Reanalysis has a spatial resolution of 200 km × 200 km over the globe. We also analyze the 1979–2008 time series of SLP and surface air temperature from an ensemble of 28 climate models participating in AMIP (*SI Appendix*, Table S2). These models use observed SSTs and sea ice as boundary conditions (37). For SSTs, we mainly rely on the NOAA Extended Reconstructed SSTs (ERSST v3b) (40). The 20th Century Reanalysis assimilated SSTs from the Hadley Center Sea Ice and Sea Surface Temperature dataset (HadISST) (41), whereas the AMIP models used SSTs from Taylor et al. (42).

We also apply the ModelE2 version of the GISS climate model (43) to examine the influence of tropical Atlantic SST on US summer air temperature. ModelE2 has a horizontal resolution of 2° × 2.5° with 40 layers extending from surface to 0.1 hPa. As done by Sutton and Hodson (16, 17), we carry out a simulation in which we force the GISS ModelE2 with idealized tropical Atlantic SST patterns, as described in *SI Appendix*. Finally, we examine results from two climate models in the CLIVAR (https://gmao.gsfc.nasa.gov/research/clivar_drought_wg/index.html). The two models, NCAR CAM3.5 and GFDL AM2.1, are forced by perturbations in tropical Atlantic SSTs (44).

Detrended data and anomalies are obtained by subtracting either the 7-y MAs or the seven-term HF trend (45). The HF is especially suited for extracting trends from seasonally varying quantities. The HF relies on a weighted MA, which can better damp irregular changes and capture turning points in trends (45). In this study, we find that use of HF can better remove the influence of abrupt emission changes than use of MA (*SI Appendix*, Fig. S26). One such abrupt change is the rapid decrease of ozone precursors in 2002 (6). Throughout this article, we specify $P < 0.05$ as the threshold for statistical significance.

ACKNOWLEDGMENTS. We thank Eric M. Leibensperger (State University of New York at Plattsburgh) for guidance in carrying out GISS ModelE2 simulations and James A. Johnstone (University of Washington) for fruitful discussion on the mechanism related to the northeast Pacific Ocean. This work was supported by the National Aeronautics and Space Administration (NASA) Air Quality Applied Sciences Team, NASA Modeling, Analysis, and Prediction Grant NNX13AO08G, NIH Grant R21ES022585, and USEPA Grant RD-83587201. Its contents are solely the responsibility of the grantee and do not necessarily represent the official views of the USEPA.

1. Cooper OR, Gao RS, Tarasick D, Leblanc T, Sweeney C (2012) Long-term ozone trends at rural ozone monitoring sites across the United States, 1990–2010. *J Geophys Res* 117:D22307.
2. Bell ML, McDermott A, Zeger SL, Samet JM, Dominici F (2004) Ozone and short-term mortality in 95 US urban communities, 1987-2000. *JAMA* 292(19):2372–2378.
3. Fishman J, Belina KM, Encarnación CH (2014) The St. Louis ozone gardens: Visualizing the impact of a changing atmosphere. *Bull Am Meteorol Soc* 95(8):1171–1176.
4. Camalier L, Cox W, Dolwick P (2007) The effects of meteorology on ozone in urban areas and their use in assessing ozone trends. *Atmos Environ* 41:7127–7137.
5. Jacob DJ, Winner DA (2009) Effect of climate change on air quality. *Atmos Environ* 43(1):51–63.
6. Bloomer BJ, Stehr JW, Piety CA, Salawitch RJ, Dickerson RR (2009) Observed relationships of ozone air pollution with temperature and emissions. *Geophys Res Lett* 36:L09803.
7. Gardner MW, Dorling SR (2000) Meteorologically adjusted trends in UK daily maximum surface ozone concentrations. *Atmos Environ* 34(2):171–176.
8. Mo KC, Thiaw WM (2002) Ensemble canonical correlation prediction of precipitation over the Sahel. *Geophys Res Lett* 29(12):1570.
9. Ndiaye O, Ward MN, Thiaw WM (2011) Predictability of seasonal Sahel rainfall using GCMs and lead-time improvements through the use of a coupled model. *J Clim* 24(7):1931–1949.
10. Seager R, Tzanova A, Nakamura J (2009) Drought in the southeastern United States: Causes, variability over the last millennium, and the potential for future hydroclimate change. *J Clim* 22(19):5021–5045.
11. Wang H, Fu R, Kumar A, Li W (2010) Intensification of summer rainfall variability in the southeastern United States during recent decades. *J Hydrometeorol* 11(4):1007–1018.
12. Kam J, Sheffield J, Wood EF (2014) Changes in drought risk over the contiguous United States (1901–2012): The influence of the Pacific and Atlantic Oceans. *Geophys Res Lett* 41:5897–5903.
13. Seager R, Hoerling M (2014) Atmosphere and Ocean Origins of North American Droughts. *J Clim* 27(12):4581–4606.
14. McCabe GJ, Palecki MA, Betancourt JL (2004) Pacific and Atlantic Ocean influences on multidecadal drought frequency in the United States. *Proc Natl Acad Sci USA* 101(12): 4136–4141.
15. Enfield DB, Mestas-Nuñez AM, Trimble PJ (2001) The Atlantic Multidecadal Oscillation and its relation to rainfall and river flows in the continental U.S. *Geophys Res Lett* 28: 2077–2088.
16. Sutton RT, Hodson DL (2005) Atlantic Ocean forcing of North American and European summer climate. *Science* 309(5731):115–118.
17. Sutton RT, Hodson DL (2007) Climate response to basin-scale warming and cooling of the North Atlantic Ocean. *J Clim* 20(5):891–907.
18. Hansen J, Sato M, Ruedy R (2012) Perception of climate change. *Proc Natl Acad Sci USA* 109(37):E2415–E2423.
19. Mo KC (2003) Ensemble canonical correlation prediction of surface temperature over the United States. *J Clim* 16(11):1665–1683.
20. Alfaro EJ, Gershunov A, Cayan D (2006) Prediction of summer maximum and minimum temperature over the central and western United States: The roles of soil moisture and sea surface temperature. *J Clim* 19(8):1407–1421.
21. Hoerling M, et al. (2013) Anatomy of an extreme event. *J Clim* 26(9):2811–2832.
22. Wang H, Schubert S, Koster R, Ham YG, Suarez M (2014) On the role of SST forcing in the 2011 and 2012 extreme US heat and drought: A study in contrasts. *J Hydrometeorol* 15(3):1255–1273.
23. Jia L, et al. (2016) The roles of radiative forcing, sea surface temperatures, and atmospheric and land initial conditions in US summer warming episodes. *J Clim* 29(11): 4121–4135.
24. McKinnon KA, Rhines A, Tingley MP, Huybers P (2016) Long-lead predictions of eastern United States hot days from Pacific sea surface temperatures. *Nat Geosci* 9(5):389–394.
25. Wilks DS (2006) *Statistical Methods in the Atmospheric Sciences*, International Geophysics Series (Academic, San Diego), Vol 59, 2nd Ed.
26. National Research Council (2010) *Committee on Assessment of Intraseasonal to Interannual Climate Prediction and Predictability, 2010* (National Academies Press, Washington, DC).
27. Lau KM, Kim KM, Shen SS (2002) Potential predictability of seasonal precipitation over the United States from canonical ensemble correlation predictions. *Geophys Res Lett* 29(7):1097.
28. Fiore AM, et al. (2009) Multimodel estimates of intercontinental sourcereceptor relationships for ozone pollution. *J Geophys Res* 114:D04301.
29. Lapina K, et al. (2014) Assessment of source contributions to seasonal vegetative expo- sure to ozone in the US. *J Geophys Res Atmos* 119:324–340.
30. Rasmussen DJ, et al. (2012) Surface ozone-temperature relationships in the eastern US: A monthly climatology for evaluating chemistry-climate models. *Atmos Environ* 47:142–153.
31. Travis KR, et al. (2016) Why do models overestimate surface ozone in the Southeast United States? *Atmos Chem Phys* 16(21):13561–13577.
32. Shen L, Mickley LJ, Tai APK (2015) Influence of synoptic patterns on surface ozone variability over the eastern United States from 1980 to 2012. *Atmos Chem Phys* 15:10925–10938.
33. Li L, Li W, Kushnir Y (2012) Variation of North Atlantic Subtropical High western ridge and its implication to the Southeastern US summer precipitation. *Clim Dyn* 39:1401–1412.
34. Gill A (1980) Some simple solutions for heat-induced tropical circulation. *Q J R Meteorol Soc* 106(449):447–462.
35. Johnstone JA, Mantua NJ (2014) Atmospheric controls on northeast Pacific temperature variability and change, 1900-2012. *Proc Natl Acad Sci USA* 111(40):14360–14365.
36. Bond NA, Cronin MF, Freeland H, Mantua N (2015) Causes and impacts of the 2014 warm anomaly in the NE Pacific. *Geophys Res Lett* 42(9):3414–3420.
37. Gates WL, et al. (1999) An overview of the results of the Atmospheric Model Intercomparison Project (AMIP I). *Bull Am Meteorol Soc* 80(1):29–55.
38. Kalnay E, et al. (1996) The NMC/NCAR CDAS/Reanalysis Project. *Bull Am Meteorol Soc* 77:437–471.
39. Compo GP, et al. (2011) The twentieth century reanalysis project. *Q J R Meteorol Soc* 137:1–28.
40. Smith TM, Reynolds RW, Peterson TC, Lawrimore J (2008) Improvements to NOAA's historical merged land-ocean surface temperature analysis (1880-2006). *J Clim* 21(10): 2283–2296.
41. Rayner NA, et al. (2003) Global analyses of sea surface temperature, sea ice, and night marine air temperature since the late nineteenth century. *J Geophys Res* 108(D14):4407.
42. Taylor KE, Williamson D, Zwiers F (2000) *The Sea Surface Temperature and Sea-Ice Concentration Boundary Conditions for AMIP II Simulations*, PCMDI Report Series (Program for Climate Model Diagnosis and Intercomparison, Livermore, CA), PCMDI Report No. 60.
43. Schmidt GA, et al. (2014) Configuration and assessment of the GISS ModelE2 contributions to the CMIP5 archive. *J Adv Model Earth Syst* 6:141–184.
44. Schubert S, et al. (2009) A US CLIVAR project to assess and compare the responses of global climate models to drought-related SST forcing patterns: Overview and results. *J Clim* 22(19):5251–5272.
45. Australian Bureau of Statistics (2003) *Information Paper: A Guide to Interpreting Time Series - Monitoring Trends* (Australian Bureau of Statistics, Canberra, Australia), Catalog No. 1349.0.